ELSEVIER

Contents lists available at ScienceDirect

Science Bulletin

journal homepage: www.elsevier.com/locate/scib



Article

Selection rules of electromagnetic transitions for chirality-parity violation in atomic nuclei

Yuanyuan Wang^a, Xinhui Wu^a, Shuangquan Zhang^{a,*}, Pengwei Zhao^a, Jie Meng^{a,b,c,*}

- ^a State Key Laboratory of Nuclear Physics and Technology, School of Physics, Peking University, Beijing 100871, China
- ^b School of Physics and Nuclear Energy Engineering, Beihang University, Beijing 100191, China
- ^c Yukawa Institute for Theoretical Physics, Kyoto University, Kyoto 606-8502, Japan

ARTICLE INFO

Article history: Received 7 July 2020 Received in revised form 3 August 2020 Accepted 17 August 2020 Available online 27 August 2020

Keywords:
Chiture
Chiplex
Spontaneously symmetry breaking
Selection rules of electromagnetic
transitions

ABSTRACT

The nuclear Chirality-Parity (ChP) violation, a simultaneous breaking of chiral and reflection symmetries in the intrinsic frame, is investigated with a reflection-asymmetric triaxial particle rotor model. A new symmetry for an ideal ChP violation system is found and the corresponding selection rules of the electromagnetic transitions are derived. The fingerprints for the ChP violation including the nearly degenerate quartet bands and the selection rules of the electromagnetic transitions are provided. These fingerprints are examined for ChP quartet bands by taking a two-j shell $h_{11/2}$ and $d_{5/2}$ with typical energy spacing for A = 130 nuclei.

© 2020 Science China Press, Published by Elsevier B.V. and Science China Press, All rights reserved.

1. Introduction

As a microscopic quantum many-body system, the atomic nucleus carries a wealth of information on fundamental symmetries and symmetry breakings which are usually manifested in energy spectra, electromagnetic transitions and their selection rules. Although the observed states preserve the symmetries of the nuclear many-body Hamiltonian, a variety of phenomena is intuitively interpreted in the intrinsic frame in which the Hamiltonian usually has less symmetry than the original one, i.e., the spontaneously symmetry breaking. For example, the spherical symmetry in atomic nuclei results in equally spaced vibration spectra, and the deviation from spherical symmetry may lead to a series of rotor-like sequences [1].

The reflection symmetry and chiral symmetry have broad interests in mathematics, physics, chemistry and biology. In nuclear physics, the reflection symmetry [2] and chiral symmetry [3] have been at the frontiers, and continue to be hot topics over the past decades, see e.g., Refs. [4–11].

In pear-shaped nuclei, the spontaneous breaking of reflection symmetry occurs and manifests itself by the occurrence of the interleaved positive and negative parity bands or a pair of parity partner bands [4,5]. The pear-shaped nuclei can provide a unique probe to test the charge-parity (CP) symmetry violation beyond

E-mail addresses: sqzhang@pku.edu.cn (S. Zhang), mengj@pku.edu.cn (J. Meng).

the standard model [12], and have attracted a lot of attentions in both nuclear physics and particle physics.

In triaxially deformed nuclei, the spontaneous breaking of chiral symmetry may occur and manifests itself by the appearance of chiral doublet bands, a pair of nearly degenerate $\Delta I=1\hbar$ bands with the same parity [3]. The coexistence of two or more chiral doublet bands in a single nucleus, i.e., multiple chiral doublets (M χ D) predicted by the microscopic covariant density functional theory [13,14], has been observed in ¹³³Ce [15], ¹⁰³Rh [16], ⁷⁸Br [17], ¹³⁶Nd [18], ¹⁹⁵Tl [19], ¹³⁵Nd [20–22], and ¹³¹Ba [23].

The observation in 78 Br, two pairs of chiral doublet bands with opposite parity connected with strong electric dipole (E1) transitions, provides the first evidence of M χ D bands in octupole soft nuclei [17]. This observation indicates that nuclear chirality can be robust against the octupole correlations, which together with the scenario in Ref. [6] encourages the exploration of the simultaneous chiral and reflection symmetry breaking in a reflectionasymmetric triaxial nucleus.

A schematic potential energy surface with simultaneous chiral and reflection symmetry breaking in the intrinsic (β_{30}, ϕ) plane is given in Fig. 1, with β_{30} the octupole deformation parameter and ϕ the azimuthal orientation angle of the total angular momentum. There are four minima corresponding to the orientation of the nuclear distribution parallel or antiparallel with the intrinsic axis, and of the angular momentum in the intrinsic frame. The symmetry restoration in the laboratory frame results in both chiral and parity splittings which give rise to four nearly degenerate states,

^{*} Corresponding author.

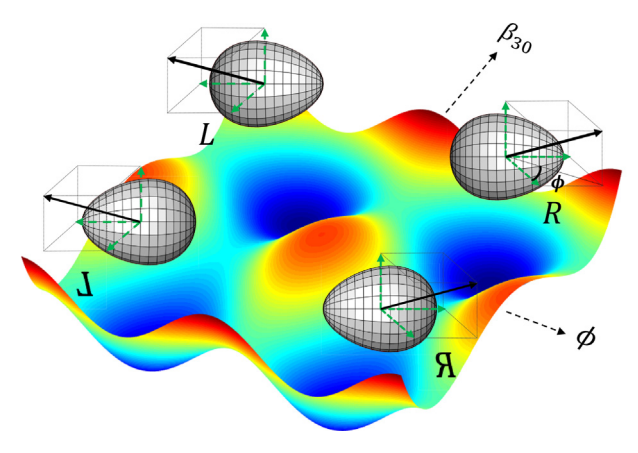


Fig. 1. (Color online) A schematic potential energy surface in the intrinsic (β_{30} , ϕ) plane for a ChP violation system, with β_{30} the octupole deformation parameter and ϕ the azimuthal orientation angle of the total angular momentum. The sign of β_{30} stands for the orientation of the nuclear distribution parallel or antiparallel with the intrinsic axis. The sign of ϕ stands for the right- and left-handed system.

i.e., chirality-parity (ChP) quartet states. The rotational excitation on the ChP quartet states will generate four nearly degenerate rotational bands, i.e., the so-called ChP quartet bands, as expected in Refs. [6,17].

In this paper, the nuclear ChP violation, a simultaneous breaking of chiral and reflection symmetries in the intrinsic frame, is investigated with a reflection-asymmetric triaxial particle rotor model (RAT-PRM). In nuclear physics, PRM takes into account a few valence particles moving in the deformed potential of the core, and to couple them to a collective rotor which stands for the rest of the particle. The energy spectra and electromagnetic transitions will be investigated, and the possible fingerprints for ChP quartet bands will be explored.

2. Ideal Chirality-Parity violation and its corresponding symmetry

The ideal chiral system prefers a maximum triaxial deformation and a pure particle-hole configuration [3]. The ideal reflection-asymmetric system requires a static octupole deformation resulting from strong octupole correlations. In order to describe the ideal ChP violation system, a RAT-PRM is developed for a core with triaxiality $\gamma=90^\circ$ coupled with one particle and one hole in a two-j shell with its orbital and total angular momenta differing by $3\hbar$, i.e., $\Delta l=\Delta j=3\hbar$.

The Hamiltonian of the core is written as

$$\widehat{H}_{\text{core}} = \frac{1}{2.7_0} \left[\widehat{R}_3^2 + 4 \left(\widehat{R}_1^2 + \widehat{R}_2^2 \right) \right] + \frac{1}{2} E(0^-) \left(1 - \widehat{P}_c \right), \tag{1}$$

where the moments of inertia for irrotational flow $\mathcal{J}_k = \mathcal{J}_0 \sin^2(\gamma - 2k\pi/3)$ are adopted, and \widehat{R}_k with k=1,2,3 represent the core angular momentum along the long, short, and intermediate axes, respectively. In Eq. (1), the core operators are rewritten as $\widehat{R}_k = \widehat{I}_k - \widehat{j}_k$, in which \widehat{I}_k and \widehat{j}_k are the angular momentum operators for the nucleus and the valence particles, respectively. The second term describes the parity splitting of the reflection-asymmetric core, with \widehat{P}_c the core parity operator and $E(0^-)$ the splitting parameter [24,25].

The intrinsic Hamiltonian for the particle moving in a reflectionasymmetric triaxially deformed potential can be written as [26]

$$\widehat{H}_{\text{s.p.}} = \hat{h}_{lj} - \hbar \omega_0 r^2 \left[\frac{\beta_{22}}{\sqrt{2}} (Y_{22} + Y_{2-2}) + \beta_{30} Y_{30} \right], \tag{2}$$

where \hat{h}_{lj} is the spherical single-particle Hamiltonian with l the orbital angular momentum and j the total angular momentum, $\hbar\omega_0 = 41A^{-1/3}$ MeV, and β_{22} and β_{30} represent the quadrupole and octupole deformation parameters, respectively. The intrinsic Hamiltonian for the hole can be obtained by changing the sign of $\hat{H}_{\text{S.D.}}[27]$.

The core Hamiltonian in Eq. (1) has good parity P_c and D_2 symmetry, i.e., the invariance with respect to rotations by π about each of the three principal axes.

The intrinsic Hamiltonian in Eq. (2) has V_4 symmetry, i.e., the invariance with respect to the reversion of the intrinsic 1 and 2 axes, while the octupole deformation breaks the intrinsic spacereflection symmetry and D_2 symmetry.

The RAT-PRM is constructed in the laboratory frame and its Hamiltonian consisting of the core and intrinsic parts has good total parity P, good angular momentum I, and V_4 symmetry. Moreover, if the two-j shell for the particle and hole is the same and the lj dependence of the corresponding \hat{h}_{lj} in Eq. (2) is neglected, the total Hamiltonian is invariant under the operation $\hat{A} = \hat{\mathcal{R}}_3(\frac{\pi}{2})\hat{C}\hat{\pi}$, with $\hat{\mathcal{R}}_3(\frac{\pi}{2})$ the rotation by $\frac{\pi}{2}$ around 3-axis, \hat{C} the exchange of particle and hole, and $\hat{\pi}$ the intrinsic space-reflection. For the reflection-symmetric system, the intrinsic Hamiltonian has good parity, the corresponding operator \hat{A} becomes $\hat{\mathcal{R}}_3(\frac{\pi}{2})\hat{C}$, which has been discussed in Ref. [28] together with the characteristic of the electromagnetic transitions for the chiral doublet bands.

The operation \hat{A} plays a role in the exchange of the right-handed system with left-handed system by the exchange of the particle and hole. The corresponding quantum number \mathcal{A} is named as "chiture", in analogy to the signature quantum number for the rotational operation $\hat{\mathcal{R}}(\pi)$. Similar to the simplex operator $\hat{\mathcal{S}} = \hat{\mathcal{R}}(\pi)\hat{P}$, a new operator $\hat{\mathcal{B}} = \hat{\mathcal{A}}\hat{P}$ is introduced and the corresponding quantum number \mathcal{B} is named as "chiplex".

3. Selection rules of electromagnetic transitions

For a given angular momentum I, the total RAT-PRM Hamiltonian $\widehat{H}_{core}+\widehat{H}_{s.p.}$ is diagonalized numerically in the strong coupling scheme as in Ref. [24]. The eigenstates of the RAT-PRM Hamiltonian can be characterized by the total parity P and the chiplex \mathcal{B} , as shown in Table 1. The corresponding chiture \mathcal{A} is given in the third column. The V_4 symmetry of the total Hamiltonian requires the projection of the core angular momentum R_3 to be even integers. For $\mathcal{A}=+1$, $\mathcal{C}\pi=+1$ or -1, and the corresponding R_3 are $0,\pm 4,\pm 8,\cdots$ or $\pm 2,\pm 6,\cdots$. For details, see Table 1. The states with same parity P but different chiture \mathcal{A} constitute the chiral doublets, and the states with same chiture \mathcal{A} but different parity P constitute the parity doublets.

The eigenstates of the RAT-PRM Hamiltonian with different angular momenta *I* are connected by electromagnetic transitions, including *E*2 and *M*1 transitions between same parity states, and *E*1 and *E*3 transitions between opposite parity states.

Table 1 Parity P and chiplex \mathcal{B} for the eigenstates of the RAT-PRM Hamiltonian. The chiture \mathcal{A} as well as possible R_3 and $C\pi$ values under V_4 symmetry is also listed.

P	\mathcal{B}	\mathcal{A}	R_3	$C\pi$
+1	+1	+1	$0,\pm 4,\pm 8\cdots$	+1
			$\pm 2, \pm 6 \cdots$	-1
	-1	-1	$0,\pm 4,\pm 8\cdots$	-1
			$\pm 2, \pm 6 \cdots$	+1
-1	+1	-1	$0,\pm 4,\pm 8\cdots$	-1
			$\pm 2, \pm 6 \cdots$	+1
	-1	+1	$0,\pm 4,\pm 8\cdots$	+1
			$\pm 2, \pm 6 \cdots$	-1

The E2 transitions can be calculated from the operator, $\hat{\mathcal{M}}(E2) = \sum_{\mu=0,\pm 2} \hat{q}_{2\mu}^{(c)}$. As the intrinsic part of $\hat{\mathcal{M}}(E2)$ is neglected, it connects states with the same C and π , i.e., $\Delta C = 0$ and $\Delta \pi = 0$. For $\gamma = 90^\circ$, the operator $\hat{q}_{20}^{(c)} \propto \beta_2 \cos \gamma$ does not contribute and thus the matrix elements between states with same R_3 vanish. Therefore, the E2 matrix elements occur only between states with different $\mathcal A$ and same $C\pi$, or in other words with different $\mathcal B$ and same $C\pi$. The M1 transitions can be calculated from the operator,

$$\hat{\mathcal{M}}(M1) = \sum_{\mu=0,\pm 1} \sqrt{\frac{3}{4\pi}} \frac{e\hbar}{2Mc} \Big[\big(g_p - g_R \big) \hat{j}_{1\mu}^p + (g_n - g_R) \hat{j}_{1\mu}^n \Big]. \tag{3} \label{eq:3}$$

If the effective gyromagnetic factor $g_{p(n)}-g_R$ is set equal to 1 for proton and -1 for neutron [3], the M1 transitions are contributed from the matrix elements between states with the same π and different C. Furthermore, the M1 operator changes R_3 by $\Delta R_3 = 0, \pm 1$. Therefore, the M1 matrix elements occur only between states with different A and A0, or in other words with different A1 and A2.

The E3 transitions can be calculated from the operator, $\hat{\mathcal{M}}(E3) = \hat{q}_{30}^{(c)}$. As the intrinsic part is neglected, one has $\Delta C = 0$ and $\Delta \pi = 0$. For the core, with the operator $\hat{q}_{30}^{(c)} \propto \beta_{30}$, the contributions are from the matrix elements between states with same R_3 . Therefore, the E3 matrix elements contribute only between states with same \mathcal{A} and $C\pi$, or in other words with different \mathcal{B} and same $C\pi$.

There is no *E*1 transitions here. For $\gamma=90^\circ$, the collective *E*1 operator $\hat{q}_{10}^{(c)}\propto\beta_2\beta_{30}\cos\gamma$ vanishes [24]. The intrinsic part does not contribute because the model space is limited to a two-*j* shell with $\Delta l=\Delta j=3\hbar$.

Starting from the yrast and yrare states, i.e., the lowest and the second lowest states, for the positive and negative parity at given I_0 , two pairs of chiral doublet bands are organized with the allowed E2 transitions between $\Delta I = 2h$ states. They constitute the ChP quartet bands, as shown in Fig. 2. The sign of the chiplex $\mathcal B$ between chiral partners is opposite, which is also true between parity partners. As the E2 transitions occur only between states with different $\mathcal B$, $\mathcal B$ changes the sign every $2\hbar$ in a band and there is no interband E2 transitions.

In Fig. 2, between states with different chiplex \mathcal{B} , the allowed M1 transitions with $\Delta I = 1\hbar$, and the allowed E3 transitions with $\Delta I = 3\hbar$ are also shown. The intraband and interband B(M1) for chiral doublet bands exhibit staggering behavior. The alternating interband E3 transitions with spin between yrast+ and yrast—might serve as a fingerprint for ChP quartet bands. Similar alternating interband E3 transitions between yrast+ and yrare—, between

yrare+ and yrast—, and between yrare+ and yrare—, are also expected.

The allowed and forbidden E2, M1, and E3 transitions for ChP quartet bands by chiplex \mathcal{B} and parity P discussed above are summarized in Table 2.

4. Chirality-Parity violation in two-j shell $h_{11/2}$ and $d_{5/2}$

The schematic energy spectra and electromagnetic transitions for the ChP quartet bands in Fig. 2 are based on the symmetry analysis, which is for the ideal case, i.e., $\gamma = 90^{\circ}$, $E(0^{-}) = 0$ MeV, the intrinsic configuration includes one particle and one hole, and the two-j shell is degenerate.

It is interesting to examine the ChP quartet bands, including their energy spectra, electromagnetic transitions and chiral geometry, if the restriction for a constant \hat{h}_{lj} in Eq. (2) is released.

For nuclei in A = 130 mass region, the two-j shell with $\Delta l = \Delta j = 3\hbar$ near the Fermi surface is $h_{11/2}$ and $d_{5/2}$, and their energy difference is taken as 0.89 MeV [29]. The other parameters adopted in RAT-PRM include the moment of inertia $\mathcal{J}_0 = 18\hbar^2/\text{MeV}$ and the parity splitting parameter $E(0^-) = 0$ MeV for the core, and the deformation parameters $\beta_{22} = 0.3$ and $\beta_{30} = 0.1$ for the intrinsic Hamiltonian.

Diagonalizing the RAT-PRM Hamiltonian, the energy spectra can be obtained. In Fig. 3, the calculated ChP quartet bands are given for $14\hbar \leqslant I \leqslant 20\hbar$ which corresponds to the region of the static chirality, where the doublet bands are nearly degenerate in energy and their electromagnetic transitions and angular momentum orientations are similar. For both the positive and negative parity, the splitting between the chiral doublet bands is less than 200 keV. The splitting between the parity doublet bands is rather small (less than 20 keV) since the core-parity splitting $E(0^-)=0$ MeV.

The electromagnetic transitions follow the features in Fig. 2. The intraband B(E2) is about one order of magnitude stronger than the interband one. Both the intraband B(M1) and the interband B(M1) exhibit staggering behavior. The alternating interband E3 transitions with spin between yrast+ and yrast— appear, in consistent with the fingerprint for ChP quartet bands. Similarities for B(E3) between yrast+ and yrare—, between yrare+ and yrast—, and between yrare+ and yrare—, are also shown.

The chiral geometry for the chiral doublet bands is usually analyzed by the composition of the angular momentum [30,31], the *K*-plot [31], the effective angles [32–34], as well as the *azimuthal plot* [34–36].

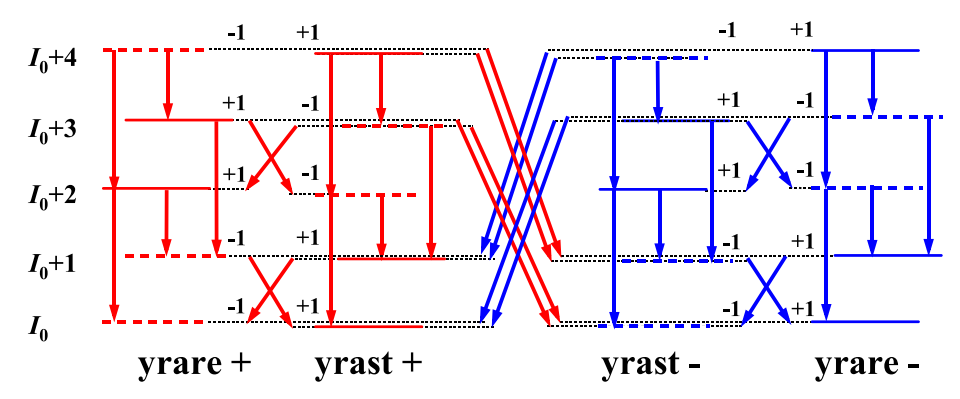


Fig. 2. (Color online) The ChP quartet bands organized by two pairs of chiral doublet bands with positive parity denoted by yrast+ and yrare+, and negative parity denoted by yrast- and yrare-. States with $\mathcal{B} = +1(-1)$ are denoted by solid (dashed) lines. Allowed E2, M1, and E3 transitions are denoted by arrows.

Table 2The electromagnetic transitions for the ChP quartet bands. The allowed transitions are denoted by " $\sqrt{}$ ", the chiplex forbidden transitions are denoted by " \times ", and the parity forbidden transitions are denoted by "-".

		$E2 \\ I \rightarrow I - 2$	$M1$ $I \rightarrow I - 1$	$M1$ $I+1 \rightarrow I$	$E3$ $I \rightarrow I - 3$	$E3 \\ I+1 \rightarrow I-2$
Intra-band	$yrast+ \rightarrow yrast+$	√	√	×	_	_
	$yrare+ \rightarrow yrare+$	\checkmark	\checkmark	×	_	_
	$yrast- \rightarrow yrast-$		\checkmark	×	_	_
	yrare− → yrare−		\checkmark	×	_	_
Inter-band	$yrast+ \leftrightarrow yrare+$	×	×	\checkmark	_	_
	yrast– ↔ yrare–	×	×		_	_
	$yrast+ \leftrightarrow yrast-$	_	_	_	\checkmark	×
	$yrare+ \leftrightarrow yrare-$	_	_	_		×
	$yrast+ \leftrightarrow yrare-$	_	_	_	×	\checkmark
	$yrare+ \leftrightarrow yrast-$	_	_	_	×	$\sqrt{}$

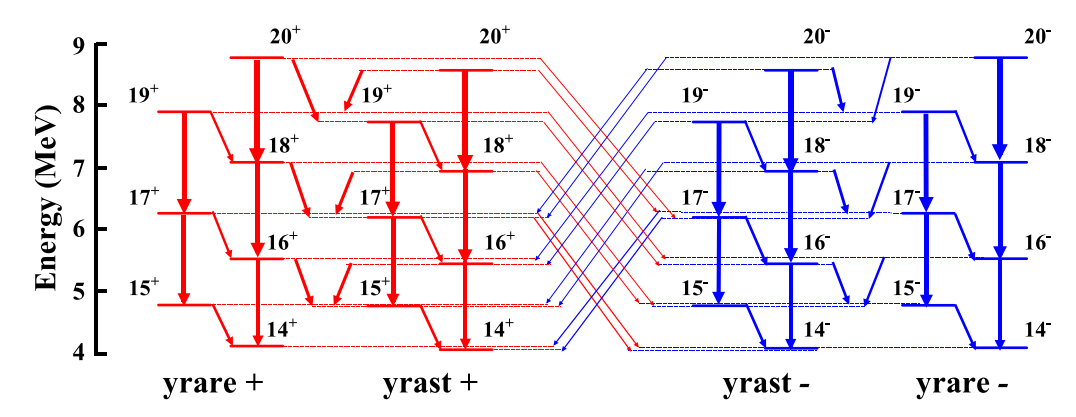


Fig. 3. (Color online) The ChP quartet bands in RAT-PRM respectively denoted by yrast+, yrare+, yrast- and yrare-. The transitions E2, M1, and E3 are denoted by arrows and the thicknesses of the arrows stand for their strength. For M1 transitions, $g_{p(n)} - g_R = 1(-1)$ is adopted.

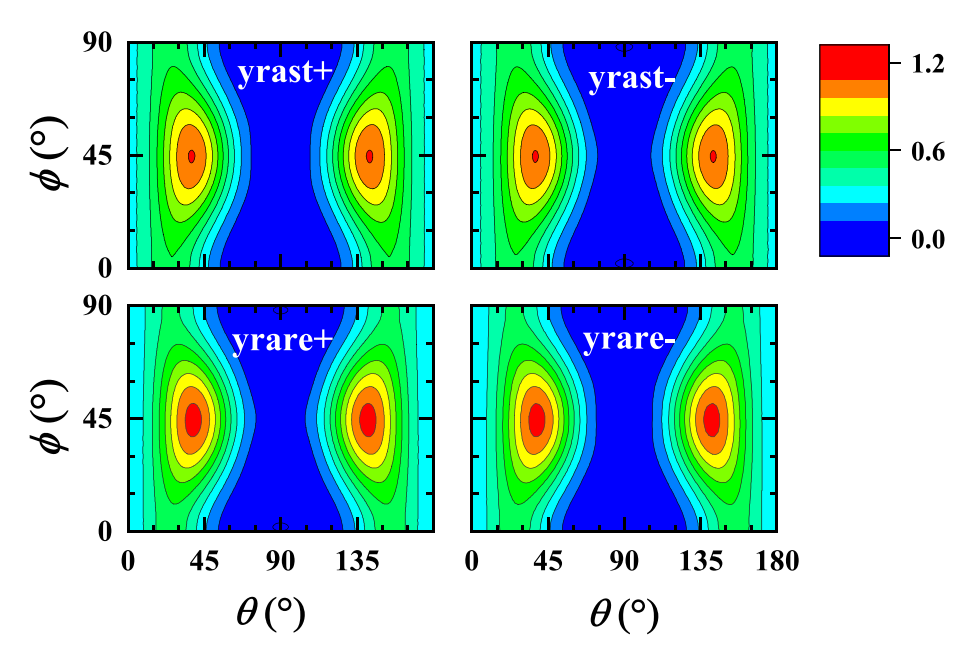


Fig. 4. (Color online) The *azimuthal plot*, i.e., the probability profile for the orientation of the angular momentum on the (θ, ϕ) plane, for ChP quartet states at $I = 16\hbar$ in RAT-PRM

The azimuthal plot provides the probability profile for the orientation of the angular momentum on the $(\theta,\,\phi)$ plane, with θ the polar angle between the angular momentum and the intrinsic 3-axis and ϕ the azimuthal angle between the projection of the angular momentum on the intrinsic 1–2 plane and the 1-axis. For

 $\gamma = 90^{\circ}$, the intrinsic 1, 2, and 3 axes are the long (*l*), short (*s*), and intermediate (*i*) axes, respectively. Accordingly, θ plays the role of ϕ in Fig. 1.

In Fig. 4, the *azimuthal plot* for ChP quartet states at $I=16\hbar$ in RAT-PRM is shown. The probability profiles for the ChP quartet

states peak at ($\phi \sim 45^{\circ}$, $\theta \sim 35^{\circ}$) and ($\phi \sim 45^{\circ}$, $\theta \sim 145^{\circ}$), demonstrating the static chirality for the chiral doublets and the near identical distribution for parity doublets.

5. Summary

In summary, the nuclear ChP violation, a simultaneous breaking of chiral and reflection symmetries in the intrinsic frame, is investigated with a RAT-PRM. The ideal ChP violation system corresponds a maximum triaxial deformation, a pure particle-hole configuration, and a static octupole deformation. The RAT-PRM Hamiltonian for the ideal ChP violation system has good total parity P, good angular momentum I, and V_4 symmetry. A new symmetry, chiture $\hat{\mathcal{A}}$ or chiplex $\hat{\mathcal{B}} = \hat{\mathcal{A}} \hat{P}$, is derived for $\gamma = 90^\circ$. The eigenstates of the RAT-PRM Hamiltonian can be characterized by the total parity P and the chiplex \mathcal{B} .

The selection rules of the electromagnetic transitions for ChP violation are revealed, and E2, M1, and E3 transitions are found to link the states with different $\mathcal B$ only. Starting from the yrast and yrare chiral doublets at I_0 for the positive parity and negative parity, the ChP quartet bands are constructed with the E2 transitions between $\Delta I = 2\hbar$ allowed. Both the intraband B(M1) and interband B(M1) exhibit staggering behavior. The interband E3 transitions alternate with spin.

The fingerprints for ChP quartet bands including the nearly degeneracy in energy and the selection rules of electromagnetic transitions are examined by taking a two-j shell $h_{11/2}$ and $d_{5/2}$ with typical energy spacing for A = 130 nuclei. The static chirality for the chiral doublets and the near identical distribution for parity doublets are demonstrated by the $azimuthal\ plot$.

Conflict of interest

The authors declare that they have no conflict of interest.

Acknowledgments

This work was partly supported by the National Natural Science Foundation of China (11875075, 11935003, 11975031, and 11621131001), the National Key R&D Program of China (2018YFA0404400 and 2017YFE0116700), the State Key Laboratory of Nuclear Physics and Technology, Peking University (NPT2020ZZ01), and the China Postdoctoral Science Foundation (2020M670014).

Author contributions

Shuangquan Zhang and Jie Meng conceived the idea and outlined the project. Yuanyuan Wang performed the calculations and drafted the manuscript together with Xinhui Wu. Shuangquan Zhang, Pengwei Zhao, and Jie Meng revised and finalized the manuscript. All authors contributed to the analysis of the results and approved the final version of the manuscript.

References

- [1] Bohr A, Mottelson BR. Nuclear structure, vol. II. World Scientific; 1975.
- [2] Bohr A. Problems of nuclear structure. Il Nuovo Cimento 1956;4:1091–120.
- [3] Frauendorf S, Meng J. Tilted rotation of triaxial nuclei. Nucl Phys A 1997;617:131–47.

- [4] Butler PA, Nazarewicz W. Intrinsic reflection asymmetry in atomic nuclei. Rev Mod Phys 1996:68:349–421.
- [5] Butler PA. Octupole collectivity in nuclei. J Phys G 2016;43:073002.
- [6] Frauendorf S. Spontaneous symmetry breaking in rotating nuclei. Rev Mod Phys 2001;73:463–514.
- [7] Meng J, Zhang SQ. Open problems in understanding the nuclear chirality. J Phys G 2010;37:064025.
- [8] Meng J, Zhao PW. Nuclear chiral and magnetic rotation in covariant density functional theory. Phys Scr 2016;91:053008.
- [9] Raduta AA. Specific features and symmetries for magnetic and chiral bands in nuclei. Prog Part Nucl Phys 2016;90:241–98.
- [10] Frauendorf S. Beyond the unified model. Phys Scr 2018;93:043003.
- [11] Xiong BW, Wang YY. Nuclear chiral doublet bands data tables. Atom Data Nucl Data Tabl 2019;125:193–225.
- [12] Gaffney LP, Butler PA, Scheck M, et al. Studies of pear-shaped nuclei using accelerated radioactive beams. Nature 2013;497:199.
- [13] Meng J, Peng J, Zhang SQ, et al. Possible existence of multiple chiral doublets in ¹⁰⁶Rh. Phys Rev C 2016;73:037303.
- [14] Zhao PW. Multiple chirality in nuclear rotation: a microscopic view. Phys Lett B 2017;773:1.
- [15] Ayangeakaa AD, Garg U, Anthony MD, et al. Evidence for multiple chiral doublet bands in ¹³³Ce. Phys Rev Lett 2013;110:172504.
- [16] Kuti I, Chen QB, Timár J, et al. Multiple chiral doublet bands of identical configuration in ¹⁰³Rh. Phys Rev Lett 2014;113:032501.
- [17] Liu C, Wang SY, Bark RA, et al. Evidence for octupole correlations in multiple chiral doublet bands. Phys Rev Lett 2016;116:112501.
- [18] Petrache CM, Lv BF, Astier A, et al. Evidence of chiral bands in even-even nuclei. Phys Rev C 2018;97:041304(R).
- [19] Roy T, Mukherjee G, Asgar MdA, et al. Observation of multiple doubly degenerate bands in ¹⁹⁵Tl. Phys Lett B 2018;782:768–72.
- [20] Zhu S, Garg U, Nayak BK, et al. A composite chiral pair of rotational bands in the odd-A nucleus ¹³⁵Nd. Phys Rev Lett 2003;91:132501.
- [21] Mukhopadhyay S, Almehed D, Garg U, et al. From chiral vibration to static chirality in ¹³⁵Nd. Phys Rev Lett 2007;99:172501.
- [22] Lv BF, Petrache CM, Chen QB, et al. Chirality of ¹³⁵Nd reexamined: evidence for multiple chiral doublet bands. Phys Rev C 2019;100:024314.
- [23] Guo S, Petrache CM, Mengoni D, et al. Evidence for pseudospin-chiral quartet bands in the presence of octupole correlations. Phys Lett B 2020;807:135572.
- [24] Wang YY, Zhang SQ, Zhao PW, et al. Multiple chiral doublet bands with octupole correlations in reflection-asymmetric triaxial particle rotor model. Phys Lett B 2019;792:454–60.
- [25] Wang YP, Wang YY, Meng J. Pseudospin symmetry and octupole correlations for MγD in ¹³¹Ba. Phys Rev C 2020;102:024313.
- [26] Wang YY, Ren ZX. Single particles in a reflection-asymmetric potential. Sci China Phys Mech Astron 2018;61:082012.
- [27] Frauendorf S, Meng J. Interpretation and quality of the tilted axis cranking approximation. Z Phys A 1996;356:263–79.
- [28] Koike T, Starosta K, Hamamoto I. Chiral bands, dynamical spontaneous symmetry breaking, and the selection rule for electromagnetic transitions in the chiral geometry. Phys Rev Lett 2004;93:172502.
- [29] Nilsson SG, Tsang CF, Sobiczewski A, et al. On the nuclear structure and stability of heavy and superheavy elements. Nucl Phys A 1969;131:1–66.
- [30] Zhang SQ, Qi B, Wang SY, et al. Chiral bands for a quasi-proton and quasineutron coupled with a triaxial rotor. Phys Rev C 2007;75:044307.
- [31] Qi B, Zhang SQ, Meng J, et al. Chirality in odd-A nucleus ¹³⁵Nd in particle rotor model. Phys Lett B 2009;675:175–80.
- [32] Wang SY, Zhang SQ, Qi B, et al. Doublet bands in ¹²⁶Cs in the triaxial rotor model coupled with two quasiparticles. Phys Rev C 2007;75:024309.
- [33] Wang SY, Zhang SQ, Qi B, et al. Description of $\pi g_{9/2} \otimes vh_{11/2}$ doublet bands in 106 Rh. Phys Rev C 2008;77:034314.
- [34] Chen QB, Meng J. Reexamine the nuclear chiral geometry from the orientation of the angular momentum. Phys Rev C 2018;98:031303(R).
- [35] Chen QB, Zhang SQ, Zhao PW, et al. Two-dimensional collective hamiltonian for chiral and wobbling modes. Phys Rev C 2016;94:044301.
- [36] Chen FQ, Chen QB, Luo YA, et al. Chiral geometry in symmetry-restored states: chiral doublet bands in ¹²⁸Cs. Phys Rev C 2017;96:051303(R).



Yuanyuan Wang received a Ph.D. degree in Particle Physics and Nuclear Physics from Beihang University in 2019. She is now working as a postdoctoral at Peking University. Her current research interest mainly focuses on nuclear structure.



Shuangquan Zhang received a Ph.D. degree in Particle Physics and Nuclear Physics from Peking University in 2002. He is now an Associate Professor of Peking University. His current research interest mainly focuses on nuclear structure as well as nuclear astrophysics.



Jie Meng received a Ph.D. degree in Theoretical Physics in 1991. He is now a Professor of Peking University. His research interest includes nuclear physics, nuclear astrophysics and many-body theory.